Laser and Particle Beams (2017), *35*, 81–91.

doi:10.1017/S0263034616000835

Stimulated Brillouin backscattering of hollow Gaussian laser beam in collisionless plasma under relativistic–ponderomotive regime

R. GAUNIYAL,[1] N. AHMAD,[2] P. RAWAT,[3] B. GAUR,[3] S.T. MAHMOUD,[2] AND G. PUROHIT[3]

[1]Uttarakhand Technical University, Dehradun, Uttarakhand 248007, India
[2]Department of Physics, College of Science, UAE University, PO Box 15551 Al-Ain, United Arab Emirates
[3]Department of Physics, Laser plasma Computational Laboratory, DAV (PG) College, Dehradun, Uttarakhand 248001, India

(RECEIVED 30 September 2016; ACCEPTED 16 November 2016)

Abstract

Stimulated Brillouin backscattering of an intense hollow Gaussian laser beam (HGLB) from collisionless plasma has been investigated under relativistic–ponderomotive regime. The main feature of considered hollow Gaussian laser beam is having the same power at different beam orders with null intensity at the center. Backscattered radiation is generated due to nonlinear interaction between main beam (pump beam) with pre-excited ion acoustic wave (IAW). Modified coupled equations has been set up for the beam width parameters of the main beam, ion-acoustic wave, back-scattered wave, and back reflectivity of stimulated Brillouin scattering (SBS) with the help of the Wentzel–Kramers–Brillouin approximation, fluid equations and paraxial theory approach. These coupled equations are solved analytically and numerically to study the laser intensity in the plasma, the variation of amplitude of the excited IAW and back reflectivity of SBS. The back reflectivity of SBS is found to be highly sensitive to the order of the HGLB, intensity of main laser beam, and plasma density for typical laser and plasma parameters. The focusing of main laser beam (hollow Gaussian) and IAW significantly affected the back reflectivity of SBS. The results show that the self-focusing and back reflectivity is enhanced for higher order modes of HGLB.

Keywords: Hollow Gaussian laser beam; Ion acoustic wave; Relativistic–ponderomotive nonlinearity; Self-focusing; Stimulated Brillouin backscattering

1. INTRODUCTION

Stimulated Brillouin back scattering (SBBS) of intense laser radiation in plasma is one of the most important parametric process, which describes the decay of the incident high power laser radiation into the scattered electromagnetic wave and an ion acoustic wave (IAW) (Kruer, 1988; Lindl *et al*., 2004). This instability is responsible for depleting and redirecting the energy flux of an incident laser wave (pump). SBBS have a great importance for inertial confinement fusion experiments (Kruer, 1995; Macgowan *et al*., 1996), because it occurs up to the critical density layer of the plasma (in the presence of ion density fluctuations) and degrades the efficiency of laser absorption in the target by reflecting a fraction of the incident energy flux. This instability also produces energetic electrons, which can preheat the target and destroys the high degree of symmetry necessary for efficient compression of the capsule (Lindl, 1995). Under fusion-relevant conditions, the energy loss by the backward SBS reflectivity (ratio of the backscattered energy on the laser beam energy) has been found to be of the order of 30%, which eventually reducing the radiation temperature in indirect drive hohlraum target (Fernández *et al*., 2006; Kline *et al*., 2006). Therefore, the suppression of SBS is of crucial importance in laser-driven inertial confinement fusion.

Stimulated Brillouin back scattering in laser–plasma interaction has been extensively studied in the past four decades when it first came to the fore in the context of fast electron generation and target preheat in laser confinement fusion. The back reflectivity of SBS is significantly affected by self-focusing (filamentation instability) of intense laser radiation and IAW in plasma (Amin *et al.,* 1993; Eliseev *et al*., 1995; Giulietti *et al*., 1999; Masson-Laborde *et al*., 2014; Purohit & Rawat, 2015). The filamentation of laser beam increases the

Address correspondence and reprint requests to: G. Purohit, Department of Physics, DAV (PG) College, Dehradun, Uttarakhand 248001, India. E-mail: gunjan75@gmail.com

local laser intensity (high-intensity filaments) and induces the SBBS in the plasma. Giulietti *et al.* (1999) have studied SBBS from underdense expanding plasma in a regime of strong filamentation and measured an extremely low back-scattering reflectivity (of the order of 10^{-4}). Sharma *et al.* (2009) investigated the effect of laser beam filamentation on the localization of IAW and on stimulated Brillouin scattering (SBS) process and observed that the intensity of IAW reduced due to enhanced Landau damping of IAW; therefore the back reflectivity of the SBS process is suppressed by a factor of approximately 10%. The influence of spatial and temporal laser beam smoothing on SBS in the presence of the filamentation instability have been investigated by Berger *et al.* (1995). The effect of diffraction on SBS from a single laser hot spot have been studied by Eliseev *et al.* (1996) and found that the SBS reflectivity from a single laser hot spot is much lower than that predicted by a simple three wave coupling model because of the diffraction of the scattered light from the spatially localized IAW. The growth of SBS process in plasma in various conditions such as laser smoothing and focusing, varying laser intensities, and plasma densities have been experimentally investigated (Fuchs *et al.*, 2000). The dependence of the SBS reflectivity on both the focusing aperture and the incident laser intensity (Baton *et al.*, 1998) has been experimentally investigated in plasma. Sodha *et al.* (1979) have studies theoretically SBS of a high-power Gaussian laser beam from a hot collisionless plasma and have shown that back reflectivity of SBS enhanced due to self-focusing of laser beam. An experimental and theoretical study of SBS using a laser pump with a duration of 8–10 ps in a laser-produced plasma has been presented by Baldis *et al.* (1993) and shown that the reflectivity is somewhat lesser than the theoretical prediction. Masson-Laborde *et al.* (2014) have observed the reduction in SBS reflectivity in laser–plasma experiments carried out by self-focusing for a single laser speckle interacting with an expanding plasma. Niknam *et al.* (2013) have investigated self-focusing and stimulated Brillouin back-scattering of a long intense laser pulse in a finite-temperature relativistic plasma considering the effects of relativistic mass and ponderomotive nonlinearities. Singh and Walia (2012) have studied the effect of self-focusing of elliptical laser beam on the Brillouin scattering process in the collisionless plasma and shows that the focusing of main beam and IAW enhanced the SBS back reflectivity. Recently, Purohit & Rawat (2015) investigated the excitation of IAW and SBBS of a ring rippled laser beam in collisionless plasma at relativistic powers, when both relativistic and ponderomotive nonlinearities are operative and observed that the back reflectivity of SBS is enhanced due to the strong coupling between ring-rippled laser beam and the excited IAW. Apart of these studies, Vyas *et al.* (2014) have reported the interplay between stimulated Raman scattering (SRS) and SBS along with the combined effect of relativistic and ponderomotive nonlinearities at relativistic laser powers within the paraxial ray approximation and found that the back reflectivity of both SRS and SBS enhanced. The other important studies of SBS process in laser–plasma interaction are found in the literature (Baton *et al.*, 1994; Asshar-Rad *et al.*, 1996; Labaune *et al.*, 1997, 2007; Mahmoud *et al.*, 1999; Mahmoud & Sharma, 2001; Singh & Walia, 2013).

It has been realized from the above studies of SBS that there is a poor agreement between theoretical and experimental results. This mismatch between the results may be due the idealized theoretical assumptions made in the theory, that is, the transverse intensity profiles of the beam have either uniform or Gaussian profile with TEM_{00} mode, but in experiment the pump beam can be superposition of the higher-order modes. Therefore, the theoretical analysis of higher-order mode of the waves is necessary for better insight of the SBS process. The back reflectivities of scattering instabilities (SRS and SBS) depend on the intensity profile of laser beam. Most of the earlier investigations have been made on SBBS process by using diversified laser beam profiles, like Gaussian, super Gaussian, ring rippled, and elliptical profiles in the presence of ponderomotive or relativistic nonlinearities. In particular, the hollow Gaussian intensity profile of a laser beam (Cai *et al.*, 2003; Misra & Mishra, 2009; Sodha *et al.*, 2009; Sharma *et al.*, 2013) is a subject of considerable interest due to its high utility in various fields (Yin *et al.*, 1998; Xu *et al.*, 2002; York *et al.*, 2008), because it can be used as an effective tool to guide, focus, and trap neutral atoms. The hollow intensity profile of Gaussian laser beam can be considered as an optical beam having null intensity at center with the same power at different beam orders, which can be produced by numerous experimental techniques (Herman & Wiggins, 1991; Wang & Littman, 1993; Lee *et al.*, 1994). When an intense laser beam propagates through the collisionless plasma, both relativistic and ponderomotive nonlinearities are simultaneously takes place. These nonlinearities depend on the time scale of laser pulse (Brandi *et al.*, 1993*a*, *b*) and modify the plasma refractive index by different mechanisms, which lead to the filamentation of the laser beam. Relativistic nonlinearity is set up due to relativistic increment in the electron mass, which increases the refractive index by decreasing the plasma frequency at higher-intensity region, which leads to relativistic self-focusing, while ponderomotive nonlinearity is set up due to the relativistic–ponderomotive force, which expels the electrons from the higher-intensity region and decreases the electron density; hence, the refractive index becomes higher at the higher-intensity region and hence enhances the self-focusing caused by the relativistic mechanism. A review of available literature highlights that the scattering instabilities (SRS and SBS) have not been investigated significantly under the relativistic–ponderomotive regime by hollow Gaussian laser beam in the plasma; except that the recent studies of stimulated Brillouin and Raman backscattering of filamented hollow Gaussian laser beam (HGLBs) in plasma (Singh & Sharma, 2013*a*, *b*).

In the present investigation, the authors have studied the evolution of HGLB collisionless plasma with relativistic and ponderomotive nonlinearities and its effect on the

https://doi.org/10.1017/S0263034616000835 Published online by Cambridge University Press

excitation of IAW and back reflectivity of SBS for different orders of self-focused HGLB. The paraxial ray approximation (Akhmanov *et al*., 1968; Sodha *et al*., 1976) is used to describe the focal region of the laser beam where all the relevant parameters correspond to a narrow range around the maximum irradiance of the HGLB. The organization of this paper is as follows:

Section 2 presents the analytical model for the propagation of HGLB in the plasma with relativistic and ponderomotive nonlinearities, generation of IAW, and for stimulated Brillouin backscattering (SBBS). Section 3 presents the numerical results and the effect of various laser–plasma parameters on the propagation of HGLB in the plasma, generation of IAW, and back reflectivity of SBS. The main conclusions are summarized in Section 4.

2. ANALYTICAL FORMULATION

2.1. Propagation of HGLB in collisionless plasma

Consider the propagation of a linearly polarized hollow Gaussian beam (HGB) with its electric vector polarized along the y-axis propagating in a homogeneous plasma along the z-axis. The electric field vector E for such a beam may be expressed in a cylindrical coordinate system with azimuthal symmetry as (Sodha *et al*., 2009)

$$E = \hat{j}E_0(r, z)\exp(i\omega_0 t), \tag{1}$$

where

$$(E_0)_{z=0} = E_{00}\left(\frac{r^2}{2r_0^2}\right)^n \exp\left(-\frac{r^2}{2r_0^2}\right). \tag{2}$$

In the above expression E_0 refers to the initial amplitude of the HGB, r_0 is the initial beam width of the beam, n is the order of the HGB and a positive integer, characterizing the shape of the HGB and position of its maximum irradiance, ω_0 is the wave frequency, $\hat{j}$ is the unit vector along the y-axis, and E_{00} is the maximum amplitude of the HGB obtained at $r = r_{\max} = r_0\sqrt{2n}$. Equation (2) represents a fundamental Gaussian beam at $n = 0$.

In the present study, we consider a plasma characterized by relativistic and ponderomotive nonlinearities. The relativistic–ponderomotive force is given by Borisov *et al.* (1992) and Brandi *et al*. (1993*a*, *b*)

$$F_{\mathrm{P}} = -m_0c^2\nabla(\gamma - 1), \tag{3}$$

where γ is the relativistic factor and is given by

$$\gamma = \left(1 + \frac{e^2}{m_0^2\omega_0^2c^2}E_0 \cdot E_0^*\right)^{1/2}. \tag{4}$$

The modified electron density due to relativistic–ponderomotive force is given by Brandi *et al*. (1993*a*, *b*)

$$n_{\mathrm{e}} = n_0 + \frac{c^2n_0}{\omega_{\mathrm{p0}}^2}\left(\nabla^2\gamma - \frac{(\nabla\gamma)^2}{\gamma}\right), \tag{5}$$

where n_0 is the background electron density of the plasma in the absence of laser beam, and

$$\begin{aligned}\frac{n_{\mathrm{e}}}{n_0} = 1 + \frac{c^2}{\omega_{\mathrm{p0}}^2}\Bigg\{&\frac{a}{r_0^2f_0^4 2^{2n}\gamma}(\eta + \sqrt{2n})^{4n}\exp[-(\eta + \sqrt{2n})^2] \\ &\times\left[\frac{8n^2}{(\eta + \sqrt{2n})^2} + 2(\eta + \sqrt{2n})^2 - 8n - 2\right] \\ &- \frac{a^2}{r_0^2f_0^6 2^{2n}\gamma^3}(\eta + \sqrt{2n})^{8n}\exp[-2(\eta + \sqrt{2n})^2] \\ &\times\left[\frac{4n^2}{(\eta + \sqrt{2n})^2} + (\eta + \sqrt{2n})^2 - 4n\right]\Bigg\}.\end{aligned} \tag{6}$$

The propagation of the HGLB in a collisionless plasma is governed by the wave equation

$$\nabla^2E_0 + \frac{\omega_0^2}{c^2}\varepsilon_0(r, z)E_0 = 0, \tag{7}$$

where ε_0 is the dielectric function of the plasma given by

$$\varepsilon_0 = 1 - \frac{\omega_{\mathrm{p0}}^2}{\omega_0^2} \tag{8}$$

with ω_{p0} $(=4\pi n_0e^2/m_0)^{1/2}$ is the plasma frequency and other symbols have their usual meaning, that is, e is the charge of an electron, m_0 is its rest mass, n_0 is the density of plasma electrons in the absence of laser beam, and c is the speed of light in free space.

Now transforming the (r, z) coordinate in to (η, z) coordinate by the relation

$$\eta = \left(\left(\frac{r}{r_0f_0}\right) - \sqrt{2n}\right), \tag{9}$$

where f_0 is the dimensionless beam width of the beam and $r = r_0f_0\sqrt{2n}$ is the position of the maximum irradiance for the propagating beam.

The effective dielectric function of the plasma in the presence of relativistic–ponderomotive nonlinearity may be given by

$$\varepsilon(r, z) = 1 - \frac{\omega_{\mathrm{p0}}^2}{\omega_0^2}\left[\frac{n_{\mathrm{e}}}{n_0\gamma}\right]. \tag{10}$$

The dielectric function $\varepsilon(\eta, z)$ around the maximum $(\eta = 0)$ of the HGB (under the paraxial like approximation) can be expressed as

$$\varepsilon(\eta, z) = \varepsilon_0(z) - \eta^2\varepsilon_2(z), \tag{11}$$

where $\varepsilon_0(z)$ and $\varepsilon_2(z)$ are the coefficients associated with η^0 and η^2 in the expansion of $\varepsilon(\eta, z)$ around $\eta = 0$

The dielectric functions $\varepsilon_0(z)$ and $\varepsilon_2(z)$ are obtained by expanding the dielectric function $\varepsilon(\eta, z)$ in the paraxial regime

https://doi.org/10.1017/S0263034616000835 Published online by Cambridge University Press

around the position of maximum intensity as

$$\varepsilon_0(z) = \varepsilon(\eta, z)_{\eta=0} = 1 - \frac{\omega_{p0}^2}{\omega_0^2}\left(\frac{1}{(1+g_0)^{1/2}}\right) + \frac{1}{\rho_0^2 f_0^2}\left(\frac{2g_0}{(1+g_0)}\right)$$

and

$$\varepsilon_2(z) = -\left(\frac{\partial\varepsilon(\eta, z)}{\partial\eta^2}\right)_{\eta=0} = \frac{\omega_{p0}^2}{\omega_0^2}\left(\frac{1}{(1+g_0)^{3/2}}\right)g_0 - \frac{1}{\rho_0^2 f_0^2}\left(\frac{4g_0^2}{(1+g_0)^2}\right),$$

where $g_0 = (a/f_0^2)n^{2n}\exp(-2n)$ and a $(=\alpha E_{00}^2)$ is the initial intensity of laser beam.

The solution of Eq. (7) can be written as

$$E_0(r, z) = \hat{j}A(r, z)\exp\left(-i\int k_0(z)dz\right), \tag{12}$$

where $A(r, z)$ is a complex amplitude of the wave and $k_0(z) = (\omega_0/c)\sqrt{\varepsilon_0(z)}$.

Substituting $E_0(r, z)$ from Eq. (12) into (7) and neglecting the term $(\partial^2 A/\partial z^2)$, one can obtain

$$2ik\frac{\partial A}{\partial z} + iA\frac{\partial k}{\partial z} = \left(\frac{\partial^2 A}{\partial r^2} + \frac{1}{r}\frac{\partial A}{\partial r}\right) + \frac{\omega^2}{c^2}(\varepsilon - \varepsilon_0)A. \tag{13}$$

The complex amplitude $A(r, z)$ may be defined as

$$A(r, z) = A_0(r, z)\exp(-ik(z)S(r, z)), \tag{14}$$

where $S(r, z)$ is the eikonal associated with the HGB and both A_0 and S are real parameters. Substituting $A(r, z)$ from Eq. (14) into (13) and separating the real and imaginary parts, one can obtain

$$\frac{2S}{k}\frac{\partial k}{\partial z} + 2\frac{\partial S}{\partial z} + \left(\frac{\partial S}{\partial r}\right)^2 = \frac{1}{k^2 A_0}\left(\frac{\partial^2 A_0}{\partial r^2} + \frac{1}{r}\frac{\partial A_0}{\partial r}\right) + \frac{\omega^2}{k^2 c^2}(\varepsilon - \varepsilon_0), \tag{15a}$$

$$\frac{\partial A_0^2}{\partial z} + A_0^2\left(\frac{\partial^2 S}{\partial r^2} + \frac{1}{r}\frac{\partial S}{\partial r}\right) + \frac{\partial A_0^2}{\partial r}\frac{\partial S}{\partial r} + \frac{A_0^2}{k}\frac{\partial k}{\partial z} = 0. \tag{15b}$$

With the help of Eq. (9), (15a) and (15b) in terms of variables (η, z) can be expressed as

$$\frac{2S}{k_0}\frac{\partial k_0}{\partial z} + 2\frac{\partial S}{\partial z} + \frac{1}{r_0^2 f_0^2}\left(\frac{\partial S}{\partial \eta}\right)^2 = \frac{1}{k_0^2 r_0^2 f_0^2 A_0}\left(\frac{\partial^2 A_0}{\partial \eta^2} + \frac{1}{(\sqrt{2n}+\eta)}\frac{\partial A_0}{\partial \eta}\right) + \frac{\omega_0^2}{k_0^2 c^2}(\varepsilon - \varepsilon_0), \tag{16a}$$

$$\frac{\partial A_0^2}{\partial \eta} + \frac{A_0^2}{r_0^2 f_0^2}\left(\frac{\partial^2 S}{\partial \eta^2} + \frac{1}{(\sqrt{2n}+\eta)}\frac{\partial S}{\partial \eta}\right) + \frac{1}{r_0^2 f_0^2}\frac{\partial A_0^2}{\partial \eta}\frac{\partial S}{\partial \eta} + \frac{A_0^2}{k_0}\frac{\partial k_0}{\partial z} = 0. \tag{16b}$$

For the paraxial ray approximation, that is, for $\eta \ll \sqrt{2n}$, the amplitude A_0 is defined as (Akhmanov *et al.*, 1968)

$$A_0^2 = \frac{E_0^2}{2^{2n} f_0^2}(\sqrt{2n}+\eta)^{4n}\exp[-(\sqrt{2n}+\eta)^2] \tag{17a}$$

and the eikonal of the pump beam is given by

$$S(\eta, z) = \frac{(\sqrt{2n}+n)^2}{2} r_0^2 f_0 \frac{df}{dz} + \varphi(z), \tag{17b}$$

where $\varphi(z)$ is a function of z and f_0 (z) is the beam width parameter for the HGB. Substituting Eqs. (17) into 16(a) and using the boundary conditions $f_0|_{z=0} = 1$ and $df_0/dz|_{z=0} = 0$, one obtains

$$\varepsilon_0 f_0 \frac{d^2 f_0}{d\xi^2} = \left(\frac{4}{f_0^2} - \rho_0^2\varepsilon_2\right), \tag{18}$$

where $\xi = (c/r_0^2\omega)z$ is the dimensionless distance of propagation and $\rho_0 = (r_0\omega/c)$ is the dimensionless initial beam width. Equation (18) describes the beam width of HGLB with the distance of propagation in a collisionless plasma, when both relativistic and ponderomotive nonlinearities are simultaneously operative.

2.2. Excitation of ion acoustic wave

The low-frequency IAW is excited due to nonlinear coupling between hollow Gaussian beam and plasma in the presence of relativistic and ponderomotive nonlinearities. This coupling arises on account of the relativistic change in the electron mass and the modification of the background electron density due to ponderomotive nonlinearity. The amplitude of IAW, which depends upon the background electron density, gets strongly coupled to the laser beam. To analyze this excitation process of IAW in the presence of ponderomotive–relativistic nonlinearity and filamented laser beam, we use the following set of fluid equations:

(i) Continuity equation:

$$\frac{\partial N_i}{\partial t} + \nabla(N \cdot V_i) = 0. \tag{19}$$

(ii) Momentum equation:

$$m\left[\frac{\partial V_i}{\partial t} + (V_i \cdot \nabla)V_i\right] = eE_i + \frac{e}{c}(V_i \times B_i) - 2\Gamma_i m_i V_i - \frac{\gamma_i \nabla P}{N}. \tag{20}$$

https://doi.org/10.1017/S0263034616000835 Published online by Cambridge University Press

The Landau damping coefficient for IAW is given by Krall & Trivelpiece (1973)

$$2\Gamma_i = \frac{\mathbf{k}}{(1+k^2\lambda_d^2)}\left(\frac{\pi k_B T_e}{8m_i}\right)^{1/2} \times\left[\left(\frac{m}{m_i}\right)^{1/2}+\left(\frac{T_e}{T_i}\right)^{3/2}\exp\left\{-\frac{T_e}{T_i(1+k^2\lambda_d^2}\right\}\right],$$

where $\lambda_d = (k_B T_0/4\pi n_0 e^2)^{1/2}$ is the Debye length and k is the wave vector of the acoustic wave. T_e and T_i are the electron and ion temperatures, E_i and B_i are associated with the electric and magnetic field vectors, and V_i is the ion fluid density. The electric field E_i is associated with the IAW and satisfies the Poisson's equation.

(iii) Poisson's equation:

$$\nabla.E_i = -4\pi(n_{es} - n_{is}), \tag{21}$$

where n_{es} and n_{is} correspond to perturbations in the electron and ion densities, and are related to each other by following equation:

$$n_{es} = n_{is}\left[1+k^2\lambda_d^2\left(\frac{n_e}{n_0\gamma}\right)\right]^{-1}. \tag{22}$$

From Eqs. (19)–(21), one obtains the general equation governing the ion density variation in the IAW as

$$\frac{\partial^2 n_{is}}{\partial t^2} + 2\Gamma_i\frac{\partial n_{is}}{\partial t} - \gamma_i v_{th}^2\nabla^2 n_{is} + \omega_{pi}^2\frac{n_e}{n_0\gamma}\frac{k^2\lambda_d^2}{1+k^2\lambda_d^2}n_{is} = 0, \tag{23}$$

where $v_{th} = \sqrt{k_B T_i/m_i}$ is the ion thermal velocity. Using the Wentzel–Kramers–Brillouin and paraxial ray approximations (Akhmanov *et al.*, 1968; Sodha *et al.*, 1976), the solution of Eq. (23) can be expressed as

$$n_{is}(r,z) = n_i(r,z)\exp[i(\omega_i t - k_i(z+S_i(r,z))], \tag{24}$$

where n_i is the slowly varying real function of r and z, S_i is the eikonal for the IAW, ω_i and k_i are the frequency and propagation constant for IAW. Substituting for n_{is} from Eq. (24) into (23) and separating real and imaginary parts, one obtains

$$2\frac{\partial S}{\partial z} + \left(\frac{\partial S}{\partial r}\right)^2 = \frac{1}{k_i^2 n_i}\left(\frac{\partial^2 n_i}{\partial r^2}+\frac{1}{r}\frac{\partial n_i}{\partial r}\right) + \frac{\omega_i^2}{k_i^2 v_{th}^2} - \left[1+\frac{\omega_i^2}{k_i^2\gamma_i v_{th}^2}\frac{n_e}{n_0\gamma}\frac{k_i^2\lambda_d^2}{1+k_i^2\lambda_d^2}\right], \tag{25}$$

$$\frac{\partial n_i^2}{\partial z^2} + \frac{\partial S}{\partial r}\frac{\partial n_i^2}{\partial r^2} + n_i^2\left(\frac{\partial^2 S}{\partial r^2}+\frac{1}{r}\frac{\partial S}{\partial r}\right) + \frac{2\Gamma_i\omega_i}{k_i\gamma_i v_{th}^2}n_i^2 = 0. \tag{26}$$

Using Eq. (9), the solution of Eqs. (25) and (26) can be written as (Singh & Sharma, 2013*a*, *b*)

$$n_i^2 = \frac{n_{i0}^2}{2^{2n}f_i^2}\left(\eta+\sqrt{2n}\right)^{4n}\left(\frac{r_0 f_0}{a_i f_i}\right)^{4n}\exp\left(-\left(\eta+\sqrt{2n}\right)^2 - 2k_d(z)\right) \tag{27}$$

and the eikonal of the IAW is

$$S_i = \left(\eta+\sqrt{2n}\right)^2\frac{r_0^2 f_0^2}{2f_i}\frac{\partial f_i}{\partial z} + \varphi(z), \tag{28}$$

where $k_d = 2\Gamma_i\omega_i/k_i\gamma_i v_{th}^2$ is the damping factor, f_i and a_i are the dimensionless beam width parameter and radius of IAW, respectively. The dimensionless beam width parameter f_i can be obtained by using the boundary condition $f_i = 1$ at $z = 0$ and $df_i/dz|_{z=0} = 0$.

$$\frac{\partial^2 f_i}{\partial\xi^2} = \left(\frac{f_i\rho_0^2}{f_0^2}\right)\left[\frac{1}{k_i^2 r_0^2 f_0^2}\left(\frac{r_0 f_0}{a_i f_i}\right)^4 - \frac{\omega_{pi}^2\lambda_d^2}{\gamma_i v_{th}^2(1+k_i^2\lambda_d^2)} \times\left(\frac{g}{(1+g)^{3/2}} - \frac{c^2}{\omega_{p0}^2 r_0^2 f_0^2}\left(\frac{4g^2}{(1+g)^2}\right)\right)\right]. \tag{29}$$

Equations (27) and (29) describe the intensity profile of IAW and dimensionless beam width parameter (f_i) of IAW respectively along with the distance of propagation in the collisionless plasma.

2.3. Stimulated Brillouin scattering

The interaction of intense HGLB (having frequency ω_0 and wave number k_0) with low-frequency IAW (having frequency ω_i and wave number k_i) generates stimulated Brillouin scattered wave of frequency ω_s and wave number k_s. The high-frequency electric field E_T can be written as a sum of the electric field E of the incident beam and E_s of the scattered wave

$$E_T = Ee^{i\omega_0 t} + E_S e^{i\omega_S t}, \tag{30}$$

where ω_0 and ω_s are the frequency of incident laser beam and scattered wave, respectively. The electric field (E_T) satisfies the wave equation

$$\nabla^2 E_T - \nabla(\nabla E_T) = \frac{1}{c^2}\frac{\partial^2 E_T}{\partial t^2} + \frac{4\pi}{c^2}\frac{\partial \mathbf{J}_T}{\partial t}. \tag{31}$$

where $\mathbf{J}_T$ is the total current density vector in the presence of the high-frequency electric field E_T. Equating the terms at scattered frequency E_S, we obtain the wave equation for scattered field that is,

$$\nabla^2 E_S + \frac{\omega_S^2}{c^2}\left[1-\frac{n_e}{n_0}\frac{\omega_p^2}{\gamma\omega_S^2}\right]E_S = \frac{1}{2}\frac{\omega_P^2}{c^2}\frac{\omega_S}{\omega_0}\frac{n^*}{n_0}E. \tag{32}$$

The solution of Eq. (33) can be written as

$$E_S = E_{S0}(r,z)e^{ik_{S0}Z} + E_{S1}(r,z)e^{-ik_{S1}Z}, \tag{33}$$

where

$$k_{S0}^2 = \frac{\omega_S^2}{c^2}\left(1-\frac{\omega_{p0}^2}{\omega_S^2}\right) = \frac{\omega_S^2}{c^2}\varepsilon_{S0},$$

https://doi.org/10.1017/S0263034616000835 Published online by Cambridge University Press

and k_{S1} and ω_S satisfy the phase-matching condition, that is,

$$k_{S1} = k_0 - k_i, \quad \omega_S = \omega_0 - \omega_i. \tag{34}$$

In Eq. (33), E_{S1} and E_{S0} are the slowly varying function of r & z and k_{S0} & k_{S1} are the propagation constant of scattered wave. From Eqs. (33) and (34), one can get

$$-k_{S0}^2 E_{S0} + 2ik_{S0}\frac{\partial E_{S0}}{\partial z} + \left(\frac{\partial^2}{\partial r^2} + \frac{1}{r}\frac{\partial}{\partial r}\right)E_{S0} + \frac{\omega_S^2}{c^2}\varepsilon_S(r,z)E_{S0} = 0, \tag{35}$$

$$-k_{S1}^2 E_{S1} - 2ik_{S1}\frac{\partial E_{S1}}{\partial z} + \left(\frac{\partial^2}{\partial r^2} + \frac{1}{r}\frac{\partial}{\partial r}\right)E_{S1} + \frac{\omega_S^2}{c^2}\varepsilon_S(r,z)$$
$$E_{S1} = \frac{1}{2}\frac{\omega_{p0}^2}{c^2}\frac{\omega_S}{\omega_0}\frac{n^*}{n_0}E_0 e^{-ik_0 S_0}, \tag{36}$$

where

$$\varepsilon_S(r,z) = \varepsilon_{S0} + \frac{\omega_{p0}^2}{\omega_S^2}\left(1 - \frac{n_e}{n_0\gamma}\right).$$

The solution of Eq. (36) may be written as

$$E_{S0} = E_{S00}(r,z)e^{ik_0 S_C}, \tag{37}$$

where E_{S00} is the real function of r and z, S_C is the eikonal for the scattered wave. Substituting Eq. (37) into (35) and separating the real and imaginary parts one can obtain

$$2\frac{\partial S_c}{\partial z} + \left(\frac{\partial S_c}{\partial r}\right)^2 = \frac{1}{k_{s0}^2 E_{S00}}\left(\frac{\partial^2 E_{S00}}{\partial r^2} + \frac{1}{r}\frac{\partial E_{S00}}{\partial r}\right) + \frac{\omega_p^2}{\varepsilon_{S0}\omega_S^2}\left(1 - \frac{n_e}{n_0\gamma}\right), \tag{38}$$

$$\frac{\partial E_{S00}^2}{\partial z} + \frac{\partial S_c}{\partial r}\frac{\partial E_{S00}^2}{\partial r} + E_{S00}^2\left(\frac{\partial^2 S_c}{\partial r^2} + \frac{1}{r}\frac{\partial S_c}{\partial r}\right) = 0. \tag{39}$$

Transforming (r, z) coordinate in to (η, z) coordinate using Eq. (9), the solution of Eqs. (38) and (39) can be written as (Singh & Sharma, 2013*a*, *b*)

$$E_{S00}^2 = \frac{B_s^2}{2^{2n} f_S^2}\left(\sqrt{2n} + \eta\right)^{4n}\left(\frac{r_0 f_0}{b f_s}\right)^{4n}\exp\left\{-\frac{r_0^2 f_0^2}{b^2 f_s^2}\left(\sqrt{2n} + \eta\right)^2\right\}$$

and

$$S_c = \frac{\left(\sqrt{2n} + \eta\right)^2}{2}\frac{r_0^2 f_0^2}{f_s}\frac{\partial f_s}{\partial z} + \phi_S(z), \tag{40}$$

where b is the initial beam width of the scattered wave, f_s is the dimensionless beam width parameter of the scattered beam, and B_s is the amplitude of the scattered beam, whose value is to be determined later by applying boundary condition.

Substituting Eq. (40) into (38) and equating the coefficient of η^2 both sides and using the boundary conditions $f_S = 1$ and $df_S/dz = 0$, we get the equation of the spot size of scattered wave

$$\frac{d^2 f_S}{d\xi^2} = \left(\frac{\rho_0^2}{f_0^2 f_s}\right)\left[\frac{1}{k_{s0}^2}\left(\frac{r_0 f_0}{b f_s}\right)^4 - \frac{\omega_s^2}{k_{s0}^2 c^2}\varepsilon_{s2}\right], \tag{41}$$

where ε_{S2} is the nonlinear dielectric constant of the scattered beam. In the presence of relativistic and ponderomotive nonlinearities, the ε_S (η, z) may be expressed as

$$\varepsilon_S(\eta, z) = \varepsilon_s(0) - \eta^2\varepsilon_{s2}, \tag{42}$$

where

$$\varepsilon_0(z) = 1 - \frac{\omega_{p0}^2}{\omega_0^2}\frac{\Omega_0^2}{(1+g_0)^{1/2}} + \frac{2g_0}{\rho_0^2(1+g_0)f_0^2},$$

$$\varepsilon_{s2} = -\left[\frac{\omega_{p0}^2}{\omega_0^2}\frac{g_0}{2(1+g_0)^{3/2}} - \frac{1}{\rho_0^2 f_0^2}\frac{4g_0^2}{(1+g_0)^2}\right].$$

The expression for B_s may be obtained by applying suitable boundary condition, that is,

$$E_S = E_{S0}(r,z)e^{ik_{S0}z} + E_{S1}(r,z)e^{-ik_{S1}z} = 0, \tag{43}$$

at $z = z_C$ (z_C is the point at which the amplitude of the scattered wave is zero). Therefore, at $z = z_C$, one can obtain

$$B_s = \frac{1}{2^{n+1}}\left(\frac{\omega_p^2}{c^2}\right)\left(\frac{n_{i0}}{n_0}\right)\left(\frac{\omega_s}{\omega_0}\right)\frac{f_S(z_c)}{f_i(z_c)f_0(z_c)}$$
$$\left(\frac{r}{a_i f_i(z_c)}\right)^{2n}\left(\frac{r}{r_0 f_0(z_c)}\right)^{2n}\left(\frac{b f_s(z_c)}{r}\right)^{2n}\left(\frac{b f_s(z_c)}{r}\right)^{2n} \tag{44}$$
$$\times\frac{E_{00}e^{-ik_d z_C}}{k_{S1}^2 - k_{s0}^2 - (\omega_p^2/c^2)\left(1 - (n_e/n_0\gamma)\right)}\frac{e^{-i(k_{S0}S_c + k_o S_0)}}{e^{i(k_{S1}z_c + k_{S0}z_c)}}$$

with the condition

$$\frac{1}{b^2 f_S^2(z_c)} = \frac{1}{r_0^2 f_0^2(z_c)} + \frac{1}{a_i^2 f_i^2(z_c)},$$

where $f_0(z_C)$, $f_i(z_C)$, and $f_s(z_C)$ are the values of dimensionless beam width parameters of pump laser beam (HGB), ion-acoustic beam, and scattered beam at $z = z_C$. The back reflectivity is defined as the ratio of the scattered wave intensity to the input pump wave intensity and is given by

$$R = \left|\frac{E_S}{E}\right|^2,$$

$$|E_S|^2 = |E_{S0}|^2 + |E_{S1}|^2 + E_{S0}E_{s0}^* e^{i(k_{S0}+k_{S1})z} + E_{S1}E_{S1}^* e^{-i(k_{S0}+k_{S1})z},$$

$$R = \frac{1}{2^{4n+2}}\left(\frac{\omega_p^2}{c^2}\right)^2\left(\frac{\omega_S}{\omega_0}\right)^2\left(\frac{n_{i0}}{n_0}\right)^2$$
$$\times\frac{(\eta + \sqrt{2n})^{8n}}{\left[k_{S1}^2 - k_{S0}^2 - \omega_{p0}^2(n_e/n_0\gamma)\right]^2}\times[I_1 + I_2 - I_3], \tag{45}$$

https://doi.org/10.1017/S0263034616000835 Published online by Cambridge University Press

where

$$I_1 = \frac{f_S^2(z_c)}{f_0^2(z_c)f_i^2(z_c)}\frac{1}{f_S^2}\left(\frac{f_0}{f_0(z_c)}\right)^{4n}\left(\frac{f_S}{f_S(z_c)}\right)^{4n}\left(\frac{r_0 f_0}{a_i f_i(z_c)}\right)^{4n} \times \exp\left[-2k_i z_c - \frac{r_0^2 f_0^2}{b^2 f_S^2}(\eta+\sqrt{2n})^2\right],$$

$$I_2 = \frac{1}{f_0^2 f_i^2}\left(\frac{r_0 f_0}{a_i f_i}\right)^{4n} \times \exp\left[-2k_i z - (\eta+\sqrt{2n})^2 - \frac{r_0^2 f_0^2}{a_i^2 f_i^2}(\eta+\sqrt{2n})^2\right],$$

$$I_3 = \frac{f_S(z_c)}{f_0(z_c)f_i(z_c)}\frac{1}{f_0 f_i f_S}\left(\frac{f_0}{f_0(z_c)}\right)^{2n}\left(\frac{f_S}{f_S(z_c)}\right)^{2n} \left(\frac{r_0 f_0}{a_i f_i(z_c)}\right)^{2n}\left(\frac{r_0 f_0}{a_i f_i}\right)^{2n}\exp[-k_i z_c - k_i z] \times \exp\left[-(\eta+\sqrt{2n})^2 - \frac{r_0^2 f_0^2}{a_i^2 f_i^2}(\eta+\sqrt{2n})^2 - \frac{r_0^2 f_0^2}{b^2 f_S^2}(\eta+\sqrt{2n})^2\right] \times \cos(k_{S1}+k_{S0})(z-z_c).$$

3. NUMERICAL RESULTS AND DISCUSSION

In order to have a numerical evaluation of the focusing of intense HGLB in plasma with relativistic–ponderomotive nonlinearity, effect of self-focused HGB on the excitation of IAW and back reflectivity of SBS, the numerical computation of Eqs. (17a), (18), (27), and (46) has been performed, respectively. These coupled equations have been solved for an initially plain wave front and obtained results with typical laser and plasma parameters; The vacuum wavelength of the laser beam (λ) = 1064 nm, the initial radius of the laser beam (r_0) = 20 μm, initial radius of the IAW (a_i) = 10 μm, $\upsilon_{th} = 0.1c$, different laser–plasma intensities ($a = 1$, 1.4, and 1.8), different orders of the HGB (n = 1, 2, and 3), and at different plasma densities ($\omega_{p0}/\omega_0 = 0.28$, 0.30, and 0.38).

The following boundary conditions are used:

$$f_0|_{z=0} = f_i|_{z=0} = f_s|_{z=0} = 1 \quad \text{and}$$
$$\left.\frac{df_0}{dz}\right|_{z=0} = \left.\frac{df_i}{dz}\right|_{z=0} = \left.\frac{df_s}{dz}\right|_{z=0} = 0.$$

Equation (18) represents the focusing/defocusing of HGLB along the distance of propagation in the plasma, while Eq. (17a) describes the intensity profile of the HGB in the plasma along the radial direction when relativistic and ponderomotive nonlinearities are operative. When the HGB propagates through a collisionless plasma, then the density of the plasma varies due to the ponderomotive force, therefore the refractive index of the plasma increases at the position of the maximum irradiance. In Eq. (18), the first term leads to the diffractional divergence of the beam, while the second term (nonlinear term) on the right-hand side of the equation is responsible for self-focusing of the beam, which arises due to the relativistic–ponderomotive nonlinearity. The beam will be focused in the plasma only when the magnitude of the nonlinear term exceeds the diverging term. The paraxial ray approximation is valid when $a < 1$; however, in the case of HGB this theory may be valid up to the extent where beam shows strong self-focusing at different order of n. Here paraxial ray approximation is known as modified paraxial-like approach (Sodha *et al.*, 2009) where $r = r_{max} = r_0\sqrt{2n}$ is the position of the maximum irradiance for the propagating beam.

The numerical calculations have been performed for different laser and plasma parameters. Figure 1a–1c show the beam width of HGB (f_0) with distance of propagation with varying the order of HGB (n), intensity of HGB (a), and plasma density (ω_{p0}/ω_0), respectively. From Fig. 1a, it is obvious that strong self-focusing occurs for higher order of the hollow Gaussian beam (n). When n increases, self-focusing length decreases and filamentation gets enhanced due to combined effect of ponderomotive and relativistic nonlinearities. This is because of the fact that ponderomotive nonlinearity enhances the self-focusing caused by relativistic nonlinearity. It is evident from Figure 1b that self-focusing of HGB in the plasma is enhanced with increase in the intensity of laser beam intensity. This is due to the fact that the nonlinear refractive terms in Eq. (18) are very sensitive to the intensity of laser beam. Therefore, as the intensity of the laser beam is increased, refractive terms become relatively stronger than diffractive terms. In addition, at high intensities of incident laser beam, more electrons contribute to self-focusing. From Figure 1c, it is found that with the increase in the value of relative plasma density beam width parameter decreases and hence self-focusing of the beam is faster. These results reflect that the propagation of HGB in collisionless plasma strongly depends on n, a, and ω_{p0}/ω_0. It is clear from Eq. (17a), the intensity profile of HGB depends on the focusing nature of HGB in plasma. Figure 2a–2c illustrate the intensity distribution of the HGLB with distance of propagation with varying the order of HGB (n), intensity of HGB (a) and plasma density (ω_{p0}/ω_0) respectively at the maximum irradiance position, that is, at $\eta = 0$, when relativistic and ponderomotive nonlinearities are operative. Due to strong self-focusing of HGB in plasma, the intensity of the HGLB also increases with increasing the parameters n, a, and ω_{p0}/ω_0. Such highly self-focused beam used for the excitation of IAW.

The IAW in plasma is excited due to nonlinear coupling with highly self-focused HGLB in the presence of relativistic and ponderomotive nonlinearities. The density profile of plasma is modified due to the ponderomotive force and relativistic effect and governed by Eq. (27). Equation (27) describes the focusing of IAW in the plasma. It is clear from Eq. (27), the intensity of IAW in plasma depends on the focusing of main HGB and IAW. We have solved Eq. (27) numerically with the help of Eq. (29) to obtain the amplitude of the density perturbation (intensity) of IAW at finite z. The results are displayed in Figure 2a–2c at the maximum irradiance position, that is, at $\eta = 0$ and the same set of parameters used in Figure 1. It is evident from the figures

https://doi.org/10.1017/S0263034616000835 Published online by Cambridge University Press

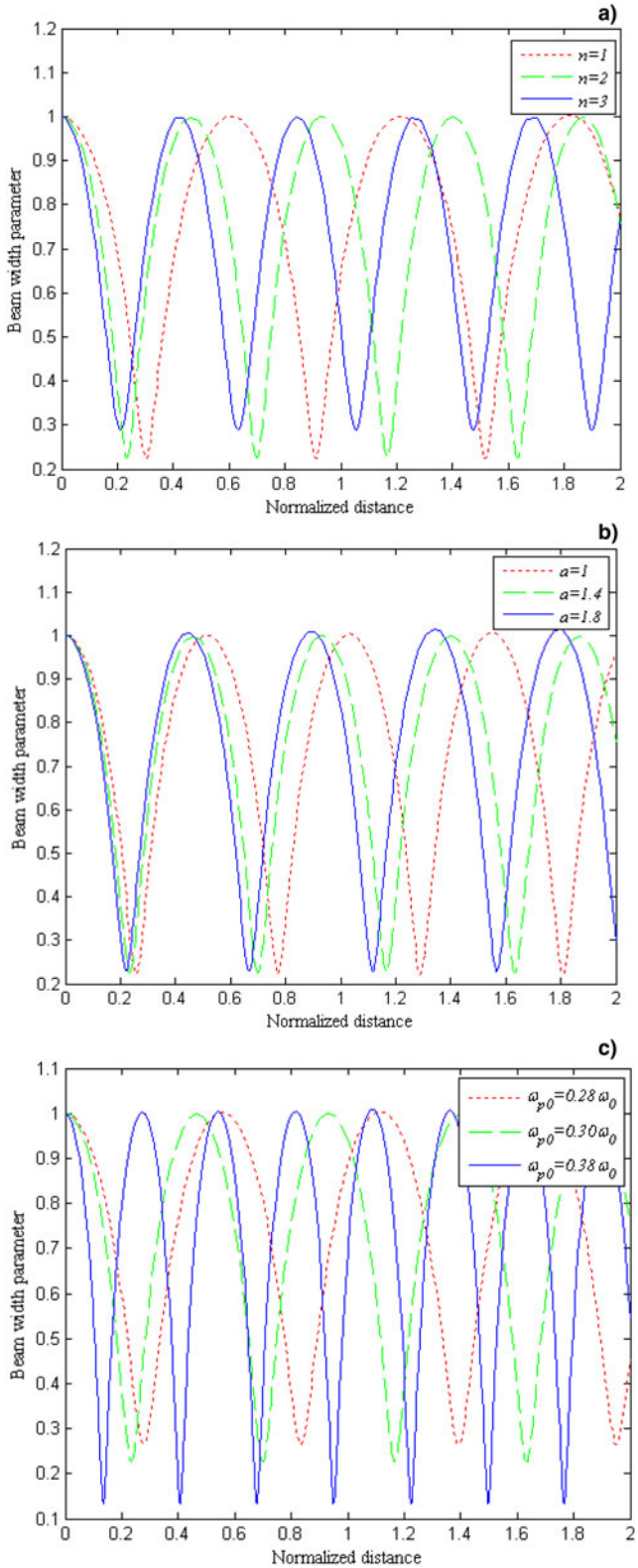

Fig. 1. Variation of beam width parameter (f_0) of HGLB with normalized propagation distance (ξ) (a) for various orders of HGB with $a = 1.4$, and $\omega_{p0} = 0.30$; (b) for different laser intensities of HGB with $n = 2$ and $\omega_{p0} = 0.30$; and (c) for different plasma densities with $a = 1.4$ and $n = 2$, when both relativistic and ponderomotive nonlinearities are taken into account.

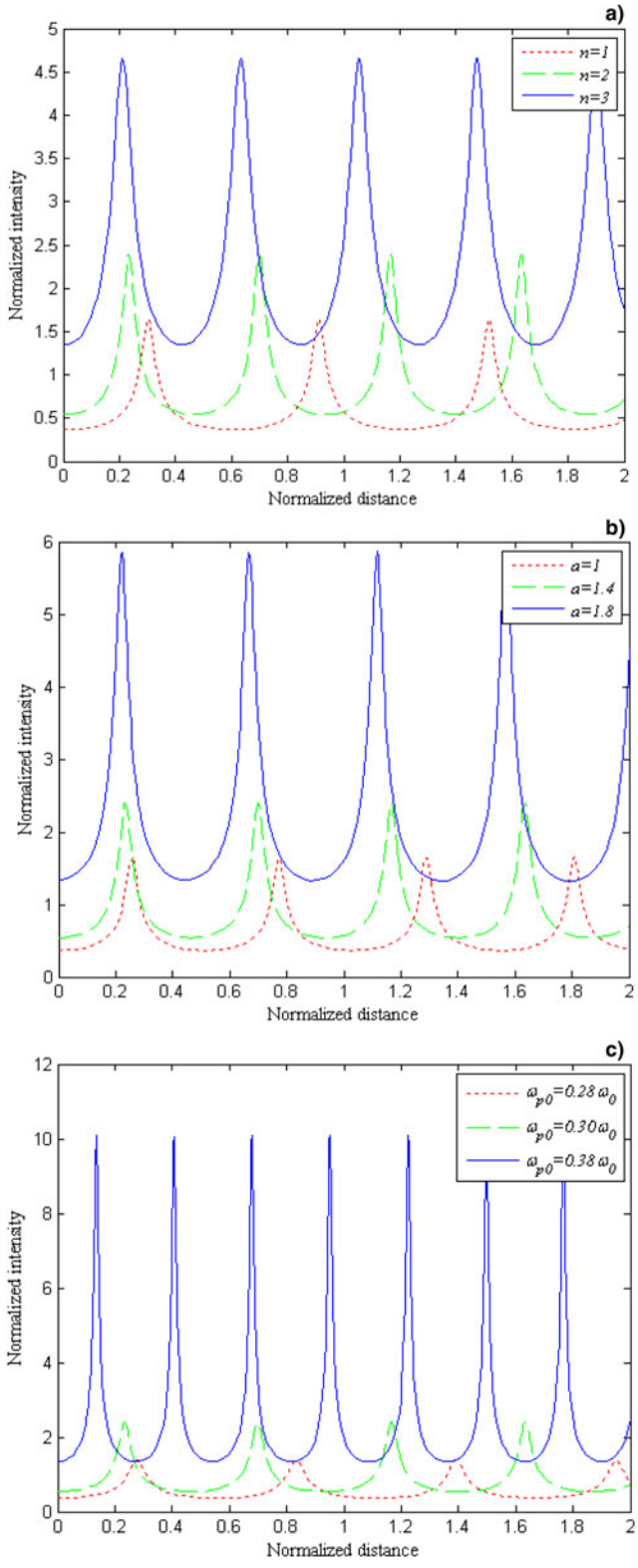

Fig. 2. Variation of laser beam intensity (HGB) in plasma with normalized distance of propagation (ξ) when relativistic and ponderomotive nonlinearities are operative. (a) For various orders of HGB with $a = 1.4$, and $\omega_{p0} = 0.30$; (b) for different laser intensities of HGB with $n = 2$ and $\omega_{p0} = 0.30$; and (c) for different plasma densities with $a = 1.4$ and $n = 2$.

https://doi.org/10.1017/S0263034616000835 Published online by Cambridge University Press

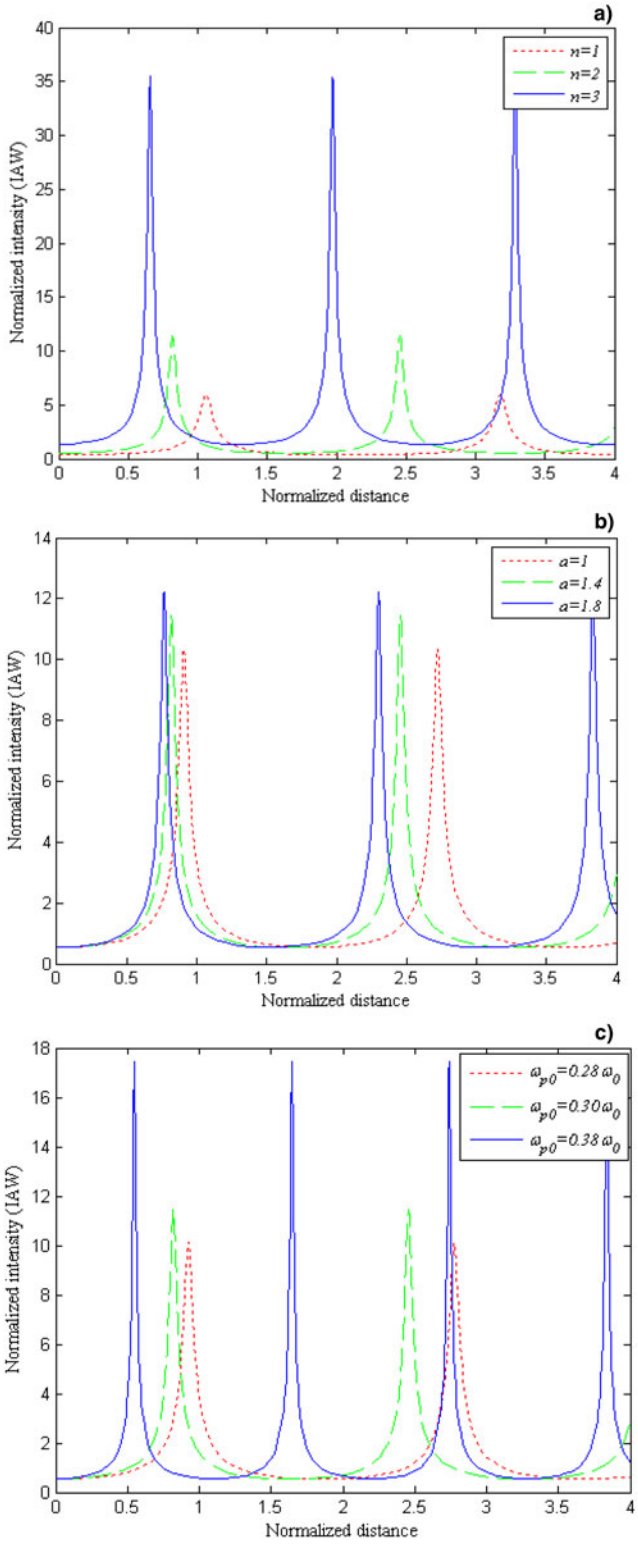

Fig. 3. Variation of IAW intensity with normalized distance of propagation (ξ): (a) for various orders of HGB with $a = 1.4$ and $\omega_{p0} = 0.30$, (b) for different laser intensities of HGB with $n = 2$ and $\omega_{p0} = 0.30$, and (c) for different plasma densities with $a = 1.4$ and $n = 2$, when both relativistic and ponderomotive nonlinearities are taken into account.

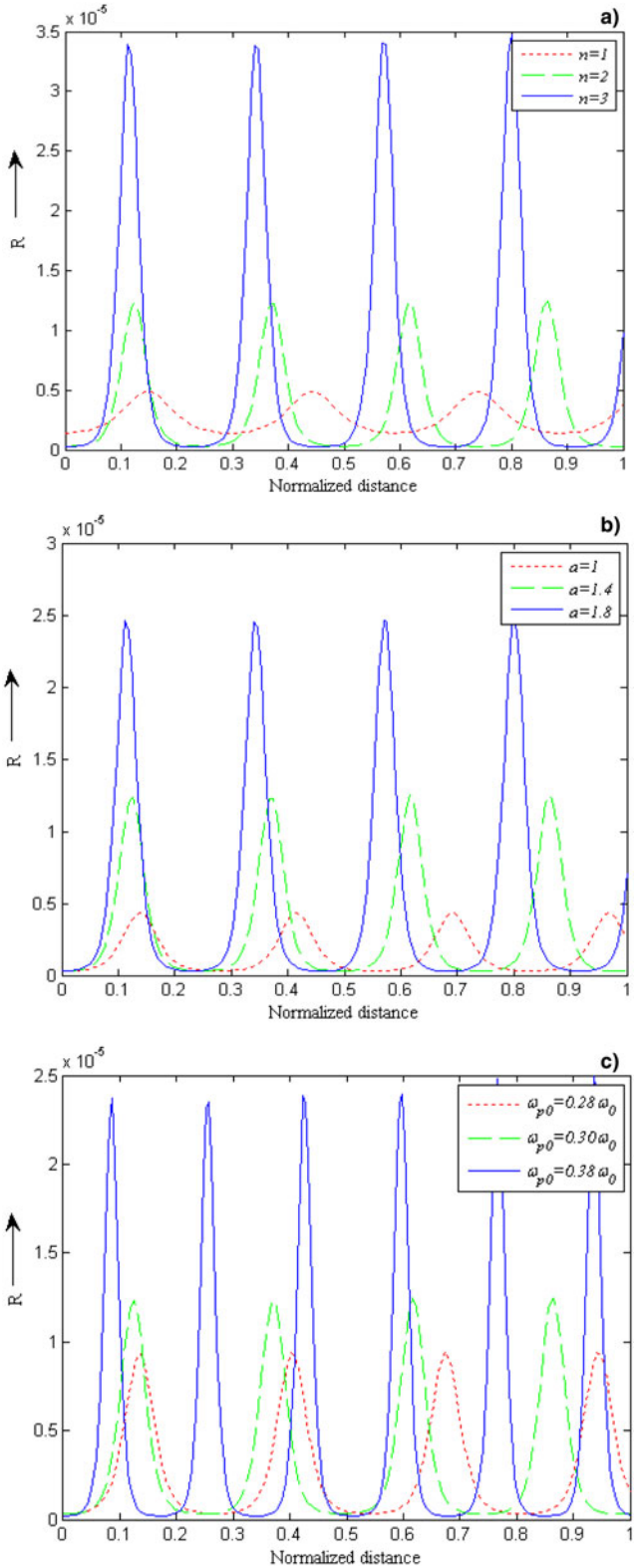

Fig. 4. Variation of back reflectivity (R) with normalized propagation distance (ξ) when relativistic and ponderomotive nonlinearities are operative. (a) For various orders of HGB with $a = 1.4$ and $\omega_{p0} = 0.30$, (b) for different laser intensities of HGB with $n = 2$ and $\omega_{p0} = 0.30$, and (c) for different plasma densities with $a = 1.4$ and $n = 2$.

https://doi.org/10.1017/S0263034616000835 Published online by Cambridge University Press

that the normalized intensity of IAW increases with increasing the order of HGB, incident laser intensity and plasma density, respectively. This is obviously due to strong self-focusing of HGLB and IAW.

In order to observe the effect of the interaction of self-focused HGLB with the low-frequency IAW in plasma on the back reflectivity of SBS process, numerical computation of Eqs. (41) and (45) has been performed for the same set of parameters used in the study of HGB and IAW. Equations (41) and (45) respectively describe the expression for the beam width parameter of the scattered beam and the back reflectivity (R) of SBS against the normalized distance of propagation. It is apparent from Eq. (45) that the reflectivity is dependent on the intensity of IAW, damping factor and beam width parameter (f_s) of the scattered beam. Figure 4a–4c represents the variation in the back reflectivity of SBS with the normalized distance of propagation. The intensity of IAW further depend on the intensity of main HGB, which get enhanced due to the filamentation process and hence the back reflectivity of SBS get enhanced with increasing n, a, and ω_{p0}/ω_0. Apart from this, back reflectivity of SBS process (in the presence of relativistic and ponderomotive nonlinearities) is inversely proportional to the beam width parameters of main HGB, IAW, and scattered beam; therefore, self-focusing of these beam enhances the back reflectivity of SBS at higher values of laser and plasma parameters used in the calculation.

4. CONCLUSIONS

In conclusion, we have studied the propagation of an intense HGLB in the collisionless plasma with relativistic and ponderomotive nonlinearities and its effect on the excitation of IAW and back reflectivity of the SBS process under the paraxial ray approximation. Effects of laser and plasma parameters such as orders of HGB, intensity of incident radiation and plasma density on the focusing of HGB, intensity of HGB and IAW as well as back reflectivity of SBS in plasma is examined. It is found that due to combined effect of relativistic and ponderomotive nonlinearities the focusing of the HGB and the intensity of HGB in a collisionless plasma is significantly enhanced for higher-order modes of the HGB. Due to strong self-focusing of HGB in the plasma, the intensity of IAW is also enhance for higher-order modes of the HGB, which significantly affected the back reflectivity of SBS. The back reflectivity increases at the focused positions for higher-order modes of HGBs because the focusing of HGB and IAW increase for higher-order modes. It is also evident from the results that the intensity of IAW and back reflectivity of SBS enhance with increasing the value of incident laser intensity. Furthermore, focusing of HGB, intensity of IAW and back reflectivity of SBS are increased by increasing the plasma density. The results show that the order of the HGLB plays very important role in the study of laser–plasma interaction. This study is useful to understand the dynamics of SBS process in laser-induced fusion where higher modes are present in the laser beam.

ACKNOWLEDGMENT

The authors are very grateful to United Arab Emirates University for financial support under grant UPAR (2014)-31S164.

REFERENCES

Akhmanov, S.A., Sukhorukov, A.P. & Khokhlov, R.V. (1968). Self-focusing and diffraction of light in a nonlinear medium. *Sov. Phys. – Usp.* **10**, 609–636.

Amin, M.R., Capjack, C.E., Frycz, P., Rozmus, W. & Tikhonchuk, V.T. (1993). Two-dimensional studies of stimulated Brillouin scattering, filamentation, and self-focusing instabilities of laser light in plasmas. *Phys. Fluids B* **5**, 3748–3764.

Asshar-Rad, T., Gizzi, L.A., Desselberger, M. & Willi, O. (1996). Effect of filamentation of Brillouin scattering in large underdense plasmas irradiated by incoherent laser light. *Phy. Rev. Lett.* **76**, 3242–3246.

Baldis, H.A., Villeneuve, D.M., LaFontaine, B., Enright, G.D., Labuane, C., Baton, S., Mounaix, Ph., Pesme, D., Casanova, M. & Rozmus, W. (1993). Stimulated Brillouin scattering in picosecond time scales: experiments and modeling. *Phys. Fluids B* **5**, 3319–3327.

Baton, S.D., Amiranoff, F., Mailka, V., Modena, A., Salvati, M., Coulaud, C., Rousseaux, C., Renard, N., Mounaix, PH. & Stenz, C. (1998). Measurement of the stimulated Brillouin scattering reflectivity from a spatially smoothed laser beam in a homogeneous large scale plasma. *Phys. Rev. E* **57**, R4895–R4898.

Baton, S.D., Rousseaux, C., Mounaix, P.H., Labaune, C., Fontaine, B., Pesme, D., Renard, N., Gary, S., Louis-Jacqet, M. & Baldis, H.A. (1994). Stimulated Brillouin scattering with a 1 ps laser pulse in a preformed underdense plasma. *Phys. Rev. E* **49**, R3602–R3605.

Berger, R.L., Lasinski, B.F., Langdon, A.B., Kaiser, T.B., Afeyan, B.B., Cohen, B.I., Still, C.H. & Willams, E.A. (1995). Influence of spatial and temporal laser beam smoothing on stimulated Brillouin scattering in filamentary laser light. *Phys. Rev. Lett.* **75**, 1078–1081.

Borisov, A.M., Borovskiy, A.V., Shiryaey, O.B., Korobkin, V.V. & Prokhorov, A.M. (1992). Relativistic and charge-displacement self-channeling of intense ultrashort laser pulses in plasmas. *Phys. Rev. A* **45**, 5830–5845.

Brandi, H.S., Manus, C. & Mainfray, G. (1993*a*). Relativistic self-focusing of ultraintense laser pulses in inhomogeneous underdense plasmas. *Phys. Rev. E* **47**, 3780–3783.

Brandi, H.S., Manus, C., Mainfray, G., Lehner, T. & Bonnaud, G. (1993*b*). Relativistic and ponderomotive self-focusing of a laser beam in a radially inhomogeneous plasma. I. Paraxial approximation. *Phys. Fluids B* **5**, 3539–3550.

Cai, Y., Lu, X. & Lin, Q. (2003). Hollow Gaussian beams and their propagation properties. *Opt. Lett.* **28**, 1084–1086.

Eliseev, V.V., Rozmus, W. & Tikhonchuk, V.T. (1996). Effect of diffraction on stimulated Brillouin scattering from a single laser hot spot. *Phys. Plasmas* **3**, 3754–3760.

Eliseev, V.V., Rozmus, W., Tikhonchuk, V.T. & Capjack, C.E. (1995). Stimulated Brillouin scattering and ponderomotive self--focusing from a single laser hot spot Phys. *Plasmas* **2**, 1712–1724.

Fernández, J.C., Goldman, S.R., Kline, J.L., Dodd, E.S., Gautier, C., Grim, G.P., Hegelich, B.M., Montgomery, D.S., Lanier, N.E., Rose, H., Schmidt, D.W., Workman, J.B., Braun, D.G.,

https://doi.org/10.1017/S0263034616000835 Published online by Cambridge University Press

Dewald, E.L., Landen, O.L., Campbell, K.M., Holder, J.P., Mackinnon, A.J., Niemann, C., Schein, J., Young, B.K., Celeste, J.R., Dixit, S.N., Eder, D.C., Glenzer, S.H., Haynam, C.A., Hinkel, D., Kalantar, D., Kamperschroer, J., Kauffman, R.L., Kirkwood, R., Koniges, A.E., Lee, F.D., Macgowan, B.J., Manes, K.R., Mcdonald, J.W., Schneider, M.B., Shaw, M.J., Suter, L.J., Wallace, R.J., Weber, F.A. & Kaae, J.L. (2006). Gas-filled hohlraum experiments at the National Ignition Facility. *Phys. Plasmas* **13**, 056319.

Fuchs, J., Labaune, C., Depierreux, S., Tikhonchuk, V.T. & Baldis, H.A. (2000). Stimulated Brillouin and Raman scattering from a randomized laser beam in large inhomogeneous collisional plasmas. I. Experiment. *Phys. Plasmas* **7**, 4659–4668.

Giulietti, A., Macchi, A., Schifano, E., Biancalana, V., Danson, C., Giulietti, D., Gizzi, L.A. & Willi, O. (1999). Stimulated Brillouin backscattering from underdense expanding plasmas in a regime of strong filamentation. *Phys. Rev. E* **59**, 1038–1046.

Herman, R.M. & Wiggins, T.A. (1991). Production and uses of diffractionless beams. *J. Opt. Soc. Am. A* **8**, 932–942.

Kline, J.L., Fernández, J.C., Goldman, S.R., Braun, D., Landen, O., Niemann, C., Gautier, D.C., Hegelich, B.M., Montgomery, D.S. & Lanier, N.E. (2006). Measurements of gas filled halfraum energetics at the national ignition facility using a single quad. *J. Phys. IV France* **133**, 919–923.

Krall, N.A. & Trivelpiece, A.W. (1973). *Principles of Plasma Physics*. New York: McGraw Hill.

Kruer, W.L. (1988). *The Physics of Laser Plasma Interactions*. New York: Addison-Wesley.

Kruer, W.L. (1995). *In Laser-Plasma Interactions 5: Inertial Confinement Fusion*. Edinburgh: SUSSP Publications.

Labaune, C., Baldis, H.A. & Tikhonchuk, V.T. (1997). Interpretation of stimulated Brillouin scattering measurements based on the use of random phase plates. *Europhys. Lett*. **38**, 31–36.

Labaune, C., Lewis, K., Bandulet, H., Depierreux, S., Huller, S., Mason-Laborde, P.E., Pesme, D. & Loiseau, P. (2007). Laser-plasma interaction in the context of inertial fusion: Experiments and modeling. *Eur. Phys. J. D* **44**, 283–288.

Lee, H.S., Stewart, B.W., Choi, K. & Fenichel, H. (1994). Holographic nondiverging hollow beam. *Phys. Rev. A* **49**, 4922–4927.

Lindl, J.D., Amendt, P., Berger, R.L., Gail Glendinning, S., Glenzer, S.H., Haan, S.W., Kauffman, R., Landen, O.L. & Suter, L.J. (2004). The physics basis for ignition using indirect-drive targets on the National Ignition Facility. *Phys. Plasmas* **11**, 339–491.

Lindl, W.L. (1995). Development of the indirect-drive approach to inertial confinement fusion and the target physics basis for ignition and gain. *Phys. Plasmas* **2**, 3933–4024.

Macgowan, B.J., Afeyan, B.B., Back, C.A., Berger, R.L., Bonnaud, G., Casanova, M., Cohen, B.I., Desenne, D.E., Dubois, D.F., Dulieu, A.G., Estabrook, K.G., Fernandez, J.C., Glenzer, S.H., Hinkel, D.E., Kaiser, T.B., Kalantar, D.H., Kauffman, R.L., Kirkwood, R.K., Kruer, W.L., Langdon, A.B., Lasinski, B.F., Montgomery, D.S., Moody, J.D., Munro, D.H., Powers, L.V., Rose, H.A., Rousseaux, C., Turner, R.E., Wilde, B.H., Wilks, S.C. & Williams, E.A. (1996). Laser–plasma interactions in ignition-scale hohlraum plasmas. *Phys. Plasmas* **3**, 2029–2040.

Mahmoud, S.T. & Sharma, R.P. (2001). Relativistic self-focusing and its effect on stimulated Raman and stimulated Brillouin scattering in laser plasma interaction. *Phys. Plasmas* **8**, 3419–3426.

Mahmoud, S.T., Sharma, R.P., Kumar, A. & Yadav, S. (1999). Effect of pump depletion and self-focusing on stimulated Brillouin scattering process in laser-plasma interactions. *Phys. Plasmas* **6**, 927–931.

Masson-Laborde, P.E., Huller, S., Pesme, D., Labaune, Ch., Depierreux, S., Loiseau, P. & Bandulet, H. (2014). Stimulated Brillouin scattering reduction induced by self-focusing for a single laser speckle interacting with an expanding plasma. *Phys. Plasmas* **21**, 032703.

Misra, S. & Mishra, S.K. (2009). Focusing of dark hollow Gaussian electromagnetic beams in a plasma with relativistic-ponderomotive regime. *Prog. Electromagn. Res. B* **16**, 291–309.

Niknam, A.R., Barzegar, S. & Hashemazadeh, M. (2013). Self-focusing and stimulated Brillouin back-scattering of a long intense laser pulse in a finite temperature relativistic plasma. *Phys. Plasmas* **20**, 122117.

Purohit, G. & Rawat, P. (2015). Stimulated Brillouin backscattering of a ring-rippled laser beam in collisionless plasma. *Laser Part. Beams* **33**, 499–509.

Sharma, A., Misra, S., Mishra, S.K. & Kourakis, I. (2013). Dynamics of dark hollow Gaussian laser pulses in relativistic plasma. *Phys. Rev. E* **87**, 063111.

Sharma, R.P., Sharma, P., Rajput, S. & Bhardwaj, A.K. (2009). Suppression of stimulated Brillouin scattering in laser beam hot spots. *Laser Part. Beams* **27**, 619–627.

Singh, A. & Walia, K. (2012). Stimulated Brillouin scattering of elliptical laser beam in collisionless plasma. *Opt. Laser Technol*. **44**, 781–787.

Singh, A. & Walia, K. (2013). Self-focusing of Gaussian laser beam in collisionless plasma and its effect on stimulated Brillouin scattering process. *Opt. Commun*. **290**, 175–182.

Singh, R.K. & Sharma, R.P. (2013*a*). Stimulated Raman backscattering of filamented hollow Gaussian beams, Laser Part. *Beams* **31**, 387–394.

Singh, R.K. & Sharma, R.P. (2013*b*) Stimulated Brillouin backscattering of filamented hollow Gaussian beams. *Laser Part. Beams* **31**, 689–696.

Sodha, M.S., Ghatak, A.K. & Tripathi, V.K. (1976). Self-focusing of laser beams in plasmas and semiconductors. *Progr. Opt*. **13**, 169–265.

Sodha, M.S., Misra, S.K. & Misra, S. (2009). Focusing of dark hollow Gaussian electromagnetic beams in a plasma. *Laser Part. Beams* **27**, 57–68.

Sodha, M.S., Umesh, G. & Sharma, R.P. (1979). Enhanced Brillouin scattering of a Gaussian laser beam from a plasma. *J. Appl. Phys*. **50**, 4678–4684.

Vyas, A., Singh, R.K. & Sharma, R.P. (2014). Combined effect of relativistic and ponderomotive filamentation on coexisting stimulated Raman and Brillouin scattering. *Phys. Plasmas* **21**, 112113.

Wang, X. & Littman, M.G. (1993). Laser cavity for generation of variable-radius rings of light. *Opt. Lett*. **18**, 767–768.

Xu, X., Wang, Y. & Jhe, W. (2002). Theory of atom guidance in a hollow laser beam: Dressed-atom approach. *J. Opt. Soc. Am. B* **17**, 1039–1050.

Yin, J., Zhu, Y., Wang, W., Wang, Y. & Jhe, W. (1998). Optical potential for atom guidance in a dark hollow laser beam. *J. Opt. Soc. Am. B* **15**, 25–33.

York, A.G., Milchberg, H.M., Palastro, J.P. & Antonsen, T.M. (2008). Direct acceleration of electrons in a corrugated plasma waveguide. *Phys. Rev. Lett*. **100**, 195001.